Bioorganic & Medicinal Chemistry Letters xxx (xxxx) xxx–xxx

Contents lists available at ScienceDirect

Bioorganic & Medicinal Chemistry Letters

journal homepage: www.elsevier.com/locate/bmcl

Biocompatible G-Quadruplex/BODIPY assembly for cancer cell imaging and the attenuation of mitochondria

Peng-Li Zhang[a], Zhuo-Kai Wang[a], Qiu-Yun Chen[a,*], Xia Du[b], Jing Gao[b]

[a] School of Chemistry and Chemical Engineering, Jiangsu University, Zhenjiang 212013, PR China
[b] School of Pharmacy, Jiangsu University, Zhenjiang 212013, PR China

ARTICLE INFO

Keywords:
BODIPY
Cancer
G4-aptamer
Mitochondria

ABSTRACT

The G-quadruplex aptamer is a high-order structure formed by folding of guanine-rich DNA or RNA. The recognition and assembly of G-quadruplex and compounds are important to find biocompatible drugs. Herein, triphenylamine conjugated 4, 4-difluoro-4-bora-3a, 4a-diaza-s-indacene (BODIPY) compound (BPTPA) was synthesized, and the interaction of BPTPA with G4 DNA was studied. It is found that BPTPA selectively binds with G_3T_3 G4 DNA forming a water-compatible nanocomplex (BPTPA-G_3T_3). BPTPA-G_3T_3 can image mitochondria and inhibit the expression of $TrxR_2$. Cytotoxicity results indicate BPTPA-G_3T_3 can decrease the membrane potential of mitochondria and inhibit the proliferation of BGC-823 cancer cells. Therefore, BPTPA-G_3T_3 can be the biocompatible attenuator of mitochondria for cancer image and chemotherapy.

Mitochondrial is the central link of all metabolic reactions in cells. They play an important role in the glucose metabolism, amino acid metabolism and fat metabolism of cancer cells.[1] Tumor cells are sensitive to disturbances of mitochondrial function. Attenuating mitochondrial dysfunction has been a strategy for cancer diagnostic and chemotherapy.[2] Mammalian thioredoxin reductase (TrxR) enzymes are overexpressed and related to the drug-resistance in cancer chemotherapy. Thus, TrxR has been reported as potential target for cancer chemotherapy.[3] Mitochondria targeting inhibitor of $TrxR_2$ can also be applied in the treatment of Parkinson's disease.[4] Liang et al reported a mitochondria targeting inhibitor of $TrxR_2$ for mitochondrial apoptosis of HeLa cancer cells. [4c]. Therefore, regulating the function of mitochondria in tumor cells and targeting inhibition of $TrxR_2$ in mitochondria will be a new method for clinical treatment of tumor cells.

It is well known that 4, 4-difluoro-4-bora-3a, 4a-diaza-s-indacene (BODIPY) derivatives can be as good bio-probes and biomaterials due to its bright fluorescence emission.[5,6] Moreover, the BODIPY core can be modified at the pyrrole ring positions, and the meso-position.[7] Triphenylamine (TPA) was commonly used as an electron donor in the design of photomaterials.[8] The combinations of TPA with conjugated π-spacer could construct compounds with good hole-transporting ability. Moreover, TPA group also was found to interact with the G-quadruple aptamers.[9] Therefore, it is possible for triphenylamine modified BODIPY bind to G-quadruple aptamer forming water compatible nanocomplex and targeting mitochondrial selectively. The G-quadruplex DNA is a high-order structure formed by folding DNA or RNA rich in tandem repeat guanine (G).[10] This type of structure is ubiquitous in the telomere end, the oncogene promoter region and the 5′UTR of mRNA, and is involved in the regulation of gene transcription.[11] Its structure is closely related to the occurrence and development of cancer. Moreover, study on the recognition and assembly of G-quadruplex with compounds would be helpful to the development of new nanodrugs or carriers for cancer diagnosis and therapy.

To develop mitochondria targeting attenuator of $TrxR_2$, triphenylamine conjugated 4, 4-difluoro-4-bora-3a, 4a-diaza-s-indacene (BODIPY) compound (BPTPA) was prepared. Furthermore, the recognition of BPTPA with G-Quadruplex aptamer (G_3T_3) makes G_3T_3 be a good carrier of BPTPA with the formation of water-compatible nanodyes (BPTPA-G_3T_3, Scheme 1). Moreover, we found that BPTPA-G_3T_3 could target mitochondria, decrease the membrane potential of mitochondria and inhibit the expression of $TrxR_2$. Study on the recognition and assembly of fluorescent compounds with G-Quadruplex aptamers provides a new method for the transfer of hydrophobic compounds into water-compatible supermolecules.

Results and discussion

The triphenylamine was introduced at the 3-sites of BODIPY resulting fluorescence BODIPY derivatives (BPTPA, Scheme S1). The

* Corresponding author.
E-mail address: chenqy@ujs.edu.cn (Q.-Y. Chen).

https://doi.org/10.1016/j.bmcl.2019.05.043
Received 2 February 2019; Received in revised form 20 May 2019; Accepted 20 May 2019

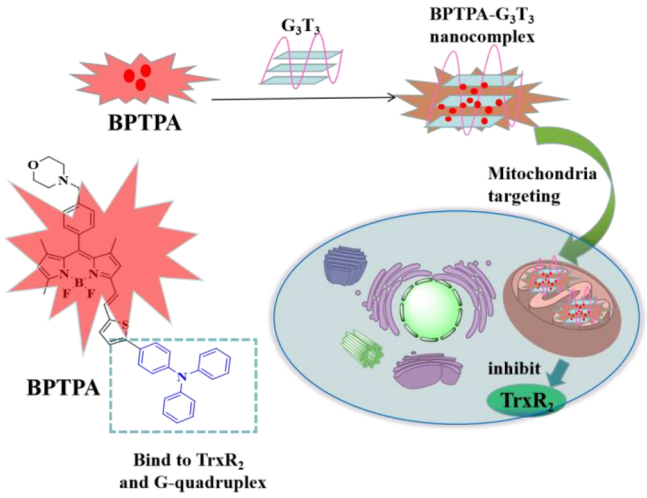

Scheme 1. Schematic illustration of BPTPA-G_3T_3 nanocomplex.

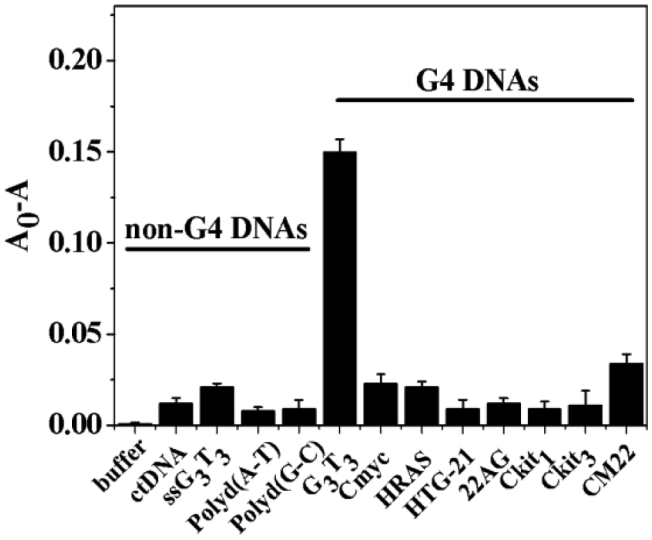

Fig. 1. The change of absorbance for BPTPA with various G4 DNAs and non-G4 DNAs in 10 mM Tris-HCl (pH 7.4, 100 mM KCl/NaCl) buffer (A_0: initial absorbance, A: final absorbance).

structure of BPTPA was characterized by ^{1}H NMR spectra, ^{13}C NMR spectra, electrospray mass spectrometry (ESI-MS) and IR spectra (Figs. S1–S3). MS (ESI$^+$, CH_3CN): Calcd for $C_{47}H_{43}BF_2N_4OS$ $[M]^+$ m/z = 759.75, found m/z = 786.84 $[(M\text{-}F)^+ + CH_3CN]^+$. ^{1}H NMR (400 MHz $CDCl_3$). δ = 7.48–7.43 (m, 4H), 7.39–7.34 (t, J = 20 Hz, 2H), 7.30–7.28 (d, J = 8 Hz, 4H), 7.13–7.11 (m, 6H), 6.93–6.91 (d, J = 8 Hz, 2H), 6.89–6.85 (m, 4H), 6.57 (s, 1H), 6.01 (s, 1H), 3.82 (s, 6H), 3.76–3.74 (t, J = 8 Hz, 4H), 2.61 (s, 6H), 2.49–2.47 (t, J = 8 Hz, 3H). ^{13}C NMR (100 MHz $CDCl_3$) δ = 152.01, 147.76, 147.38, 146.16, 141.47, 140.89, 133.78, 129.90, 129.75, 129.39, 129.07, 128.92, 128.71, 127.93, 126.66, 124.71, 123.42, 123.32, 123.22, 122.84, 118.00, 117.87, 66.82, 63.00, 53.47, 22.23, 14.63. The characteristic peaks of BPTPA at 2924 cm^{-1} (C—H stretching vibrations), 1465 cm^{-1} (C=C stretching vibrations), 1375 cm^{-1} (C—N stretching vibrations), 1182 cm^{-1} (C—C stretch), 1080 cm^{-1} (C—O stretch) and 966 cm^{-1} (Ar-H bending vibrations) were observed for BPTPA. As shown in Fig. S4, BPTPA had the highest absorbance in CH_2Cl_2. The maximum UV–vis absorption of BPTPA is 618 nm in CH_2Cl_2. The BPTPA is red shift due to the π-π^* transition. The maximum emission wavelength of BPTPA is 699 nm (Fig. S5). Therefore, BPTPA is a near-infrared fluorescent compound.

It is reported that aptamers (such as, G_3T_3, HRAS, HTG-21, et al see Table S1) can form G-quadruple structures in the presence of 10 mM Tris-HCl (pH 7.4, 100 mM KCl/NaCl) buffer.[12] In order to select a G-quadruplex aptamer that binds to BPTPA, we determined the change of absorbance of BPTPA after addition of various G-quadruplexes (Fig. 1). It was found that BPTPA selectively binds well to G_3T_3 with G-quadruplex structure, while it show weak interaction with other aptamers, single strand G_3T_3 (ssG_3T_3), linear duplex (ctDNA), and self-complementary duplex strands (polyd(A-T), polyd(G-C)). To investigate the binding of BPTPA with G_3T_3, we determined the UV titration spectra of G_3T_3 to BPTPA and calculated its binding constant (Fig. 2a and b). The results indicated that the absorbance of BPTPA decreases with the increasing amount of G_3T_3. Moreover, BPTPA exhibited higher binding affinity to G_3T_3 than other G-quadruple DNA in Table 1. The effect of BPTPA on the conformation of G_3T_3 G4-DNA was investigated by using circular dichroism (CD) assessments. As shown in Fig. 2c, in the presence of 10 mM K^+ ions, G_3T_3 was of the typical anti-parallel G-quadruplex structure, with a major positive band at 289 nm and a negative peak at ~240 nm[13,14]. Upon the addition of BPTPA to the G_3T_3 solution, there was no significant change in the structure of G_3T_3 G4-DNA. It indicates that BPTPA binds to G_3T_3 G4-DNA without changing the conformation of G_3T_3 G4-DNA. To get more details about the interaction of BPTPA with G_3T_3, molecular docking was performed to obtain detection models and binding free energies of BPTPA by Poisson-Boltzmann surface area (MM/PBSA) calculations (Fig. 3a). From the BPTPA-G_3T_3 molecular model, the binding pattern of BPTPA to G_3T_3-G4 DNA was the groove binding mode. In addition, BPTPA exhibited a superior binding energy (-88.3264 kcal/mol). Spectroscopic titration and docking calculation results demonstrate that BPTPA and G_3T_3 G4-DNA can be well combined. TEM shows the formation of BPTPA-G_3T_3 nanosheet (Fig. 3b). Therefore, BPTPA was specifically combined with G_3T_3 G4-DNA resulting water compatible BPTPA-G_3T_3 nanocomplex based on their self-assembly.

When BGC-823 cells treated with BPTPA and BPTPA-G3T3, the strong cellular fluorescence was observed (Fig. 4b). Electron micrographs of the cells provided direct evidence that BPTPA-G3T3 can enter BGC-823 cells. Next, the mitochondrial target imaging of BPTPA-G3T3 was evaluated by comparison with the mitochondria targeting dye, Mito Tracker Green FM. The yellow overlapped images of Mito Tracker Green FM and BPTPA-G3T3 in the cell demonstrate that BPTPA-G3T3 can enter mitochondria. The observed clear image and cell shapes indicate that BPTPA-G3T3 is a good mitochondrial targeting probe. In contrast, unclear images and precipitations were observed when the BPTPA was added into cells because of its low water solubility. To further investigate the effect of BPTPA-G_3T_3 on mitochondria, we monitored the mitochondrial membrane potential of BPTPA-G_3T_3 treated BGC-823 cells using a fluorescent and voltage-sensitive dye JC-1.[15] As shown in Fig. 5a, the change in red/green fluorescence ratio directly reflects changes in mitochondrial membrane potential. Different concentrations of BPTPA-G_3T_3 were added to BGC-823 cells for 24 h. As the concentration of BPTPA-G_3T_3 increased, JC-1 dye exhibited progressively enhanced green fluorescence intensity and decreased red fluorescence intensity indicating

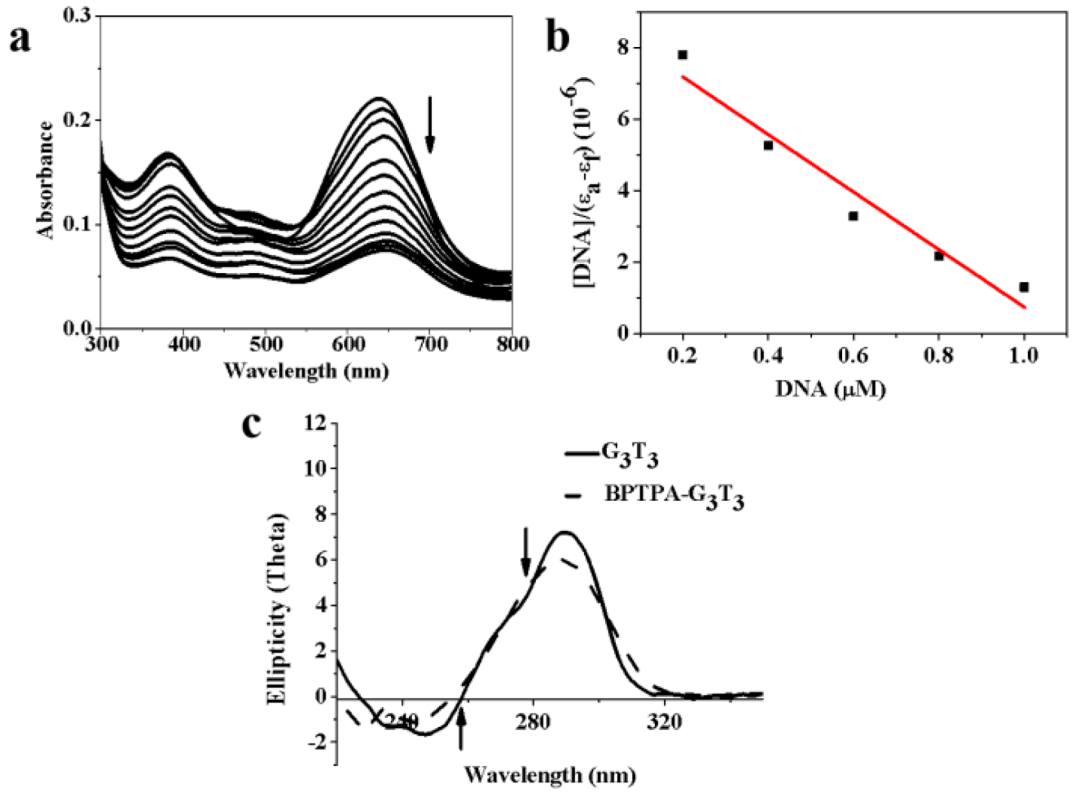

Fig. 2. (a) UV–vis spectra of BPTPA in buffer (10 mM Tris–HCl, pH 7.4, 100 mM KCl) in the presence of increasing amounts of G_3T_3 G4-DNA. BPTPA = 10 μM, [G_3T_3] = 0–1 μM from top to bottom. (b) The plot of [DNA]/(ε_a-ε_f) versus [DNA] for the titration. (c) CD spectra of G_3T_3 G4-DNA (1 μM) and BPTPA-G_3T_3 ([BPTPA] = 10 μM, [G_3T_3] = 1 μM) in buffer (10 mM Tris-HCl, pH 7.4, 100 mM KCl).

Table 1
Apparent binding constants (Ka) of G-quadruplex DNA, determined from Ultraviolet titrations.

G-quadruplex DNA	Ka [10^6 M^{-1}]
22AG	0.087
CM22	0.246
Cmyc	0.158
$Ckit_1$	0.069
$Ckit_3$	0.077
HTG-21	0.068
HRAS	0.143
G_3T_3	0.915

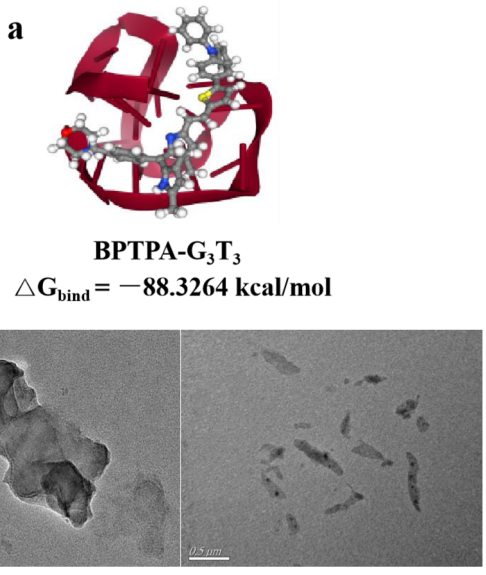

Fig. 3. (a) The complex model of G_3T_3 G4-DNA with BPTPA. (b) TEM images of BPTPA-G_3T_3.

that the mitochondrial potential was decreased. This result demonstrates that BPTPA-G_3T_3 is the attenuator of the mitochondrial functions. The rapid metabolism of cancer cells makes them more susceptible to mitochondrial perturbations.[16] The mitochondria of cancer cells are different from normal cells in structures and functions, such as the molecular composition of the mitochondrial inner membrane and mitochondrial membrane penetration.[2] Mitochondrial dysfunction is involved in the apoptotic process and energy metabolism of malignant cells.[17] The cytotoxicity of BPTPA-G_3T_3 was determined by MTT method to study its inhibition to the growth of cancer cells (BGC-823, Patu 8988 and MCF-7 cell lines, Figs. 4a and S6). Results show that BPTPA-G_3T_3 has a concentration-dependent cytotoxicity on BGC-823 cells, but has little effect on Patu 8988 and MCF-7. So we selected BGC-823 gastric cancer cells for next experiments." The IC_{50} value of BPTPA-G_3T_3 to BGC-823 cells was 31.5 ± 0.4 μmol/L. Therefore, BPTPA-G_3T_3 can be a mitochondrial attenuator and has a good inhibitory effect on cancer cell growth.

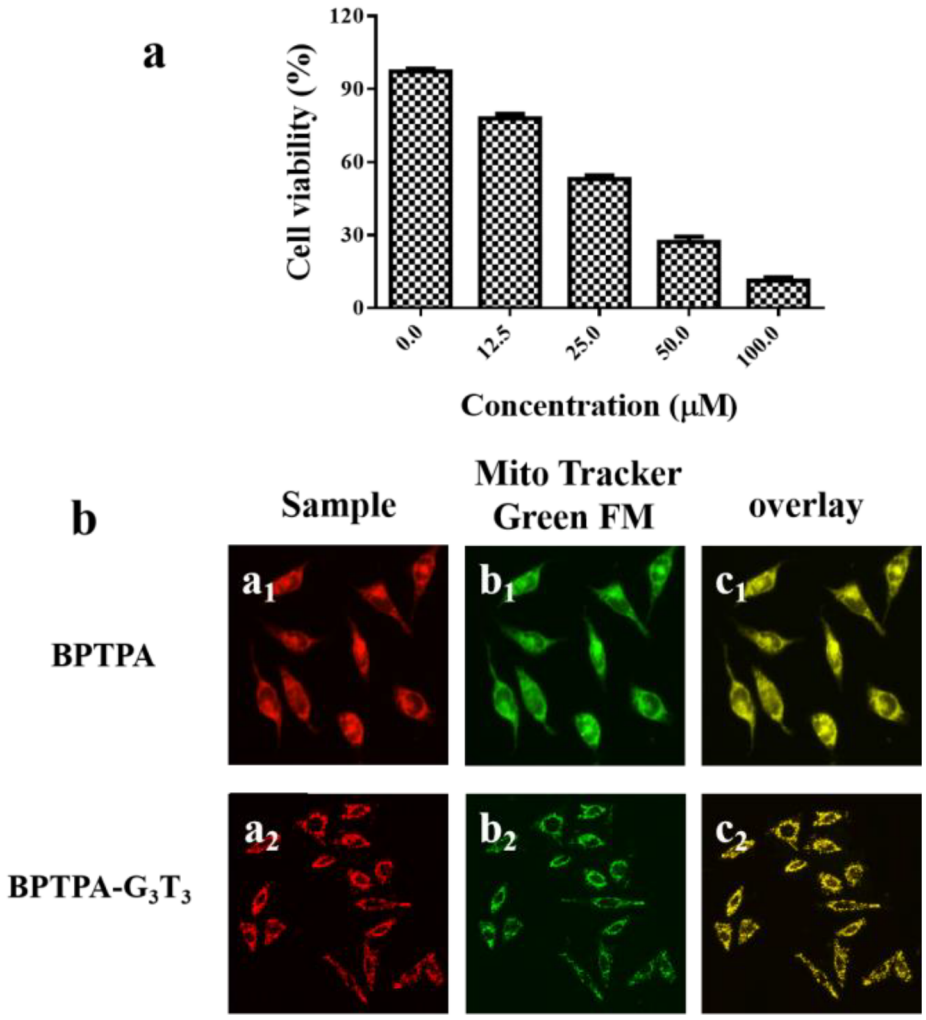

Fig. 4. (a) Inhibition activities of BPTPA-G3T3 on the proliferation of BGC-823 cells. [G3T3] = 0 μM, 1.25 μM, 2.5 μM, 5 μM, 10 μM. (b) Fluorescence image in BGC-823 cells. (a1-2) Sample imaging (2 μM) [G3T3] = 0.2 μM, 0.4 μM; (b1-2) Mito Tracker Green FM imaging; (c1-3) overlapped imaging of sample and Mito Tracker Green FM.

Thioredoxin reductase (TrxR) is a member of the family of antioxidant systems widely distributed in organisms. It is responsible for the regulation of enzymes and transcription factors and redox states at the cellular level, and is involved in cell growth, proliferation and apoptosis.[18] There are three isozymes in TrxR, of which $TrxR_2$ is mainly distributed in mitochondria. Studies have found that $TrxR_2$ is overexpressed in cancer tissues promoting cancer cell proliferation.[19,20] To study the effect of the mitochondria targeting BPTPA on the expression of $TrxR_2$, the expression of $TrxR_1$ and $TrxR_2$ in BGC-823 cells after incubated with BPTPA-G_3T_3 were carried out and compared with BDP-M (a similar BODIPY derivative, structure and toxicity were shown in Scheme S1 and Fig. S7, respectively).[21] The high expression of $TrxR_1$ and $TrxR_2$ in BGC-823 cells can be detected after incubated with BDP-M indicating BODIPY structure has less contribution to the inhibition; in contrast, BPTPA-G_3T_3 shows good inhibition on the expression of mitochondrial $TrxR_2$ (Figs. 5b and S8). It indicates that the triphenylamino group of the BPTPA plays key role to the inhibition of $TrxR_2$. This further shows that BPTPA-G_3T_3 can selectively target subcellular mitochondria and induce mitochondrial dysfunction by attenuating the mitochondrial potential and inhibiting the expression of $TrxR_2$.

In conclusion, the triphenylamino group conjugated BODIPY derivatives (BPTPA) was synthesized and assayed for its interactions with G-quadruple aptamers. It is found that BPTPA can bind to G-quadruple aptamer (G_3T_3) forming water-compatible nanosheet (BPTPA-G_3T_3). Live cell imaging showed that BPTPA-G_3T_3 could carry BPTPA to mitochondria and decrease the membrane potential of mitochondria. Mitochondria play an important role in tumorigenesis. BPTPA-G_3T_3 can attenuate mitochondrial function and inhibit the expression of mitochondrial $TrxR_2$. Therefore, BPTPA-G_3T_3 can inhibit cancer cell growth. The recognition and assembly of fluorescent compound BPTPA and G-Quadruplex aptamer G_3T_3 provide a new method for the transfer of hydrophobic compounds into mitochondrial targeting water-compatible supermolecules for cancer diagnostic and attenuation in future.

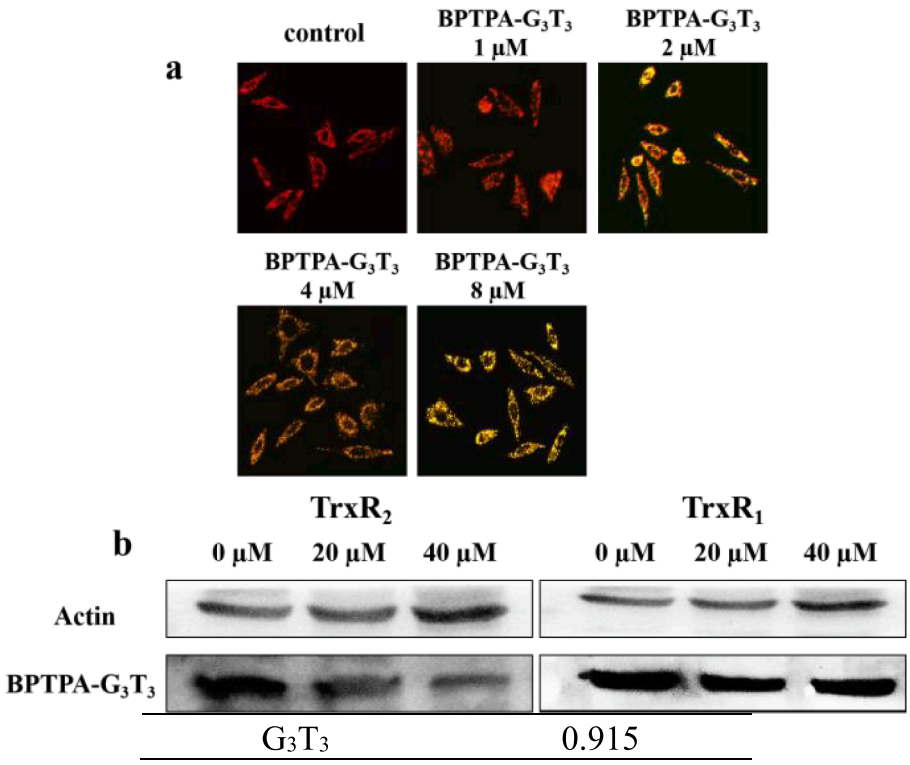

Fig. 5. (a) Fluorescence imaging of mitochondrial membrane potential in the presence different concentrations of BPTPA-G_3T_3. [G_3T_3] = 0 μM, 0.1 μM, 0.2 μM, 0.4 μM, 0.8 μM. (b) The expression of $TrxR_1$ and $TrxR_2$ in BGC-823 cells after incubated with BPTPA-G_3T_3 for 24 h. [G_3T_3] = 0 μM, 2 μM, 4 μM.

Acknowledgment

This work was financially supported by the National Natural Science Foundation of China (21571085, 21271090).

Appendix A. Supplementary data

Supplementary data to this article can be found online at https://doi.org/10.1016/j.bmcl.2019.05.043.

References

1. Liang BX, Shao WY, Zhu CG, et al. *Biol.* 2016;11:425–434.
2. (a) Yang R, Mu WY, Chen QY, Wang Q, Gao J, Biomater ACS. *Sci Eng.* 2018;4:2606–2613;
   (b) Sanjiban C, Shama PK, Rana PS. *Mitochondrion.* 2018;43:25–29.
3. (a) Holmgren A, Lu J. *Biochem Biphys Res Commun.* 2010;396:120–124;
   (b) Lu J, Holmgren A. *Free Radical Biol Med.* 2014;66:5–87;
   (c) Lincoln DT, Ali EE, Tonissen KF, Clarke FM. *Anticancer Res.* 2002;23:2425–2433.
4. (a) Liu YP, Ma HL, Zhang LW, Cui YJ, Liu XT, Fang JG. *Chem Commun.* 2016;52:2296–2299;
   (b) Folda A, Citta A, Scalcon V, et al. *Sci Rep.* 2016;6:23071.
5. (a) Verwilst P, Kim HR, Seo JH, Sohn NW, Cha SY, Kim YM, et al. *J Am Chem Soc.* 2017;139:13393–13403;
   (b) Li Z, Zhu ZZ, Shu ZW, Ding J, You JM. *Sens Actuators B Chem.* 2019;282:541–548.
6. (a) Bacalum M, Wang L, Boodts S, Yuan PJ, Leen VK, Smisdom N, et al. *Langmuir.* 2016;32:3495–3505;
   (b) Zhang PL, Shao J, Li XT, Chen QY, Qu LL. *Anal Methods.* 2019;11:827–831.
7. (a) Ozdemir T, Bila JL, Sozmen F, Yildirim LT, Akkaya EU. *Org Lett.* 2016;18:4821–4823;
   (b) Zhang JX, Wang L, Xie ZG, Biomater ACS. *Sci Eng.* 2018;4:1969–1975.
8. (a) Cui YH, Li P, Song CP, Zhang HY. *J Phys Chem C.* 2016;120:28939–28950;
   (b) Liu WS, Zheng XY, Liu JQ, et al. *J Alloys Comp.* 2017;718:379–385.
9. Wang MQ, Liu S, Tang CP. *Dyes Pigm.* 2017;136:78–84.
10. Keniry MA. *Biopolymers.* 2000;56:123–146.
11. Patel DJ, Phan AT, Kuryavyi V. *Nucleic Acids Res.* 2007;35:7429–7455.
12. Wang MQ, Zhu WX, Song ZZ, Li S, Zhang YZ. *Bioorg Med Chem Lett.* 2015;25:5672–5676.
13. Mu WY, Yang R, Robertson A, Chen QY. *Colloids Surf. B: Biointerfaces.* 2018;162:427–431.
14. Hu MH, Chen SB, Guo RJ, Ou TM, Huang ZS, Tan JH. *Analyst.* 2015;140:4616–4625.
15. Guo D, Bi H, Liu B, Wu Q, Wang D, Cui Y. *Toxicol In Vitro.* 2013;27:731–738.
16. Ralph SJ, Rodríguezenríquez S, Neuzil J, Sánchez RM. *Mol Aspects Med.* 2010;31:29–59.
17. D'Souza GGM, Wagle MA, Saxena V. *Biochim Biophys Acta, Mol Cell Biol Lipids.* 2011;1807:689–696.
18. Dagnell M, Pace PE, Cheng Q. *J Biol Chem.* 2017;292:14371–14380.
19. Yan J, Xu J, Fei Y, et al. *Exp Cell Res.* 2016;344:67–75.
20. Fisher-Wellman KH, Mattox TA, Thayne K, et al. *J Physiol.* 2013;591:3471–3486.
21. Biyiklioglu Z, Barut B, Ozel A. *Dyes Pigments.* 2018;148:417–428.